AIP CONFERENCE PROCEEDINGS 275

ATOMIC PHYSICS 13

THIRTEENTH INTERNATIONAL CONFERENCE ON ATOMIC PHYSICS

MUNICH, GERMANY 1992

EDITORS:

H. WALTHER
T. W. HÄNSCH
B. NEIZERT
MAX PLANCK INSTITUTE
FOR QUANTUM OPTICS
GARCHING, GERMANY
AND
LUDWIG MAXIMILIAN UNIVERSITY
MUNICH, GERMANY

AIP

American Institute of Physics **New York**

LONG-LIVED RESONANT STATES IN PLANETARY ATOMS

K. Richter and D. Wintgen
Fakultät für Physik, Hermann-Herder-Str. 3, 7800 Freiburg, FRG

ABSTRACT

We report on a class of long-lived resonant states of doubly excited two-electron atoms which exhibit distinct angular and radial electron correlation. The states are characterized by a highly polarized inner electron located near the axis between the nucleus and a *dynamically* localized outer electron. Classical mechanics studies prove the stability of the corresponding classical motion and allow for EBK-quantization to obtain semiclassical energies. The resonance states are treated further within the framework of a single channel adiabatic approximation. The adiabatic energies as well as the semiclassical results are in good agreement with resonance energies obtained by highly accurate solutions of the full three-body Schrödinger equation. Approximate quantum numbers derived from the semiclassical and from the adiabatic approach explain the nodal structures of the full quantum wavefunctions. The decay widths of the resonances turn out to be extremely small.

I. INTRODUCTION

The non-separability of the three-body Coulomb problem becomes evident in the case of highly doubly-excited atoms or ions, where the electron-electron interaction is of comparable importance to the electron-ion interaction. The effect of inter-electron repulsion, i.e. electron correlation, typically leads to the breakdown of independent particle approaches and has focused interest on the search for approximate symmetries using collective coordinates of the three particles. Thus the structure and formation of highly correlated electronic states is of topical interest in spectroscopy [1, 2, 3, 4] and theoretical atomic physics [5, 6, 7, 8].

Due to the intrinsic non-separability of the problem, there exists no global classification scheme which allows an overall description of the huge variety of doubly-excited states occurring. In this contribution we report on a novel class [9, 10] of strongly correlated electron states (*"Planetary Atom"* states [11]) which do not fit any of the known classification schemes proposed in the literature. The states are composed of a strongly polarized (inner) electron located along the axis connecting the nucleus and the outer electron which is *dynamically* localized near some fixed radial distance. Thus both electrons are located on the same side of the nucleus (in contrast to "symmetric" collinear configurations with both electrons on different sides of the nucleus which are associated with *intra-shell* resonances [7, 12]). The resonance states have the following pronounced properties:

(i) distinct angular and radial correlations,

(ii) no (bound) independent particle limit (nuclear charge $Z = \infty$),

(iii) quasi-separability of the wavefunctions in collective semiclassical and molecular coordinates,

(iv) extremely small (particle-) decay widths.

These states exhibit their typical features for excitiations which would correspond to independent particle principal quantum numbers $N > 5$ of the inner electron. Thus the states belong to an energy regime which is characterized by a vast number of overlapping resonances and interacting Rydberg series.

In the following we apply classical, semiclassical and quantum mechanical (approximate adiabatic and large-scale *ab initio*) methods to investigate these states.

II. (SEMI-)CLASSICAL DYNAMICS

We first give a classical analysis of the relevant electron pair motion to get insight into the underlying dynamical properties.

The non-relativistic Hamiltonian of a two-electron atom (or ion) with charge Z and nuclear mass $M = \infty$ is given by (atomic units used)

$$H = \frac{\mathbf{p}_1^2 + \mathbf{p}_2^2}{2} - \frac{Z}{r_1} - \frac{Z}{r_2} + \frac{1}{r_{12}} . \tag{1}$$

r_1 and r_2 are the electron distances from the nucleus, and r_{12} is the inter-electron distance.

We will focus on states with total angular momentum $\mathbf{L}=0$. Then the motion is confined to a fixed plane in configuration space and the Hamiltonian reduces essentially to three (coupled) degrees of freedom.

Consider a collinear arrangement of a nucleus Z and of two electrons, both being on the same side of the nucleus. The fundamental periodic motion of such a configuration is a coherent oscillation of both electrons with the same frequency but, as it turns out, with large differences in their individual radial amplitudes and velocities as depicted in figure 1(a) for helium ($Z=2$): The outer electron appears to stay nearly frozen at some fixed radial distance. The localization of the outer electron is a pure dynamical effect due to electron correlation.

The significance of a periodic orbit for the corresponding quantized system depends essentially on the structure of the classical phase space in the vicinity of the orbit [13]. The periodic trajectory of figure 1(a) is linearly stable with respect to variations in the initial conditions. This is demonstrated in figure 1(b), which shows the resulting regular motion of the electrons when they are initially in a slightly off-collinear arrangement. The inner electron then moves on perturbed Kepler ellipses around the nucleus, while the outer electron remains trapped at large radial distances following the slow angular precession of the inner electron.

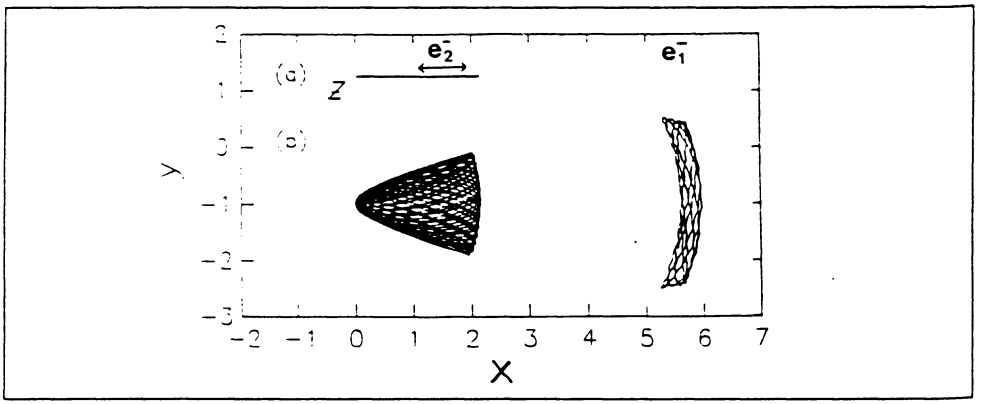

Figure 1: The radial extents of the electrons for (a) the periodic trajectory, and (b) a nonperiodic but regular trajectory in its neighborhood.

The localization of the outer electron rests upon the inter–electron repulsion for small distances of the electrons and upon the asymptotical dominance of the nuclear attraction. A careful analysis of the classical mechanics reveals that the fundamental periodic mode is embedded in a fully six–dimensional island of stability in classical phase space. This implies the near–integrability of the three–body Coulomb problem for asymmetric configurations as shown in fig. 1.

A semiclassical treatment of the classical motion suggests the existence of a Rydberg series of resonances converging to the three–particle breakup threshold [14].

$$E_{nkl} = -\frac{S^{sc2}}{(n+\frac{1}{2}+2(k+\frac{1}{2})\gamma_1+(l+\frac{1}{2})\gamma_2)^2}\,. \tag{2}$$

S^{sc}=1.49150 is the (scaled) action of the periodic orbit of figure 1 for helium. γ_1=0.46164 and γ_2=0.06765 are the classical winding numbers. The Rydberg series is characterized by three quantum numbers n, k, l which are to be interpreted as nodal excitations along the orbit (n) and along the two directions perpendicular to the orbit, the bending degree of freedom (k) and the motion perpendicular to the orbit preserving collinearity (l). The semiclassical quantum numbers n, k and l reflect the approximate separability of the associated semiclassical wavefunctions in the local coordinates parallel and perpendicular to the periodic orbit.

III. ADIABATIC APPROXIMATION

A striking property of the classical periodic orbit of figure 1 is the large difference in the electronic velocities. This indicates that an adiabatic quantum mechanical treatment similar to the Born–Oppenheimer (BO) approximation in molecular physics should be applicable. We use the axis $\mathbf{r}_1$ between the nucleus and the outer electron as adiabatic coordinate. A detailed description of our

adiabatic method can be found in Ref. [10].

As a first step the Schrödinger equation has to be solved for the inner electron in the field of the two fixed Coulomb centers with charges Z and -1 and distance $R = r_1$. As is well known from molecular physics [15] this Schrödinger equation is separable in prolate spheroidal coordinates λ, μ, which for our coordinates read

$$\lambda = \frac{r_2 + r_{12}}{R}, \qquad \mu = \frac{r_2 - r_{12}}{R}. \tag{3}$$

The resulting molecular orbital (MO) eigenfunctions ϕ for the inner electron separate in prolate spheroidal coordinates, $\phi(\lambda, \mu; R) = \xi_{n_\lambda}(\lambda)\eta_{n_\mu}(\mu)$. (The azimuthal quantum number m of the MO functions is zero for $\mathbf{L} = 0$.) The function $\xi_{n_\lambda}(\lambda)$ has elliptical nodal surfaces with the nucleus and the outer electron as foci. The function $\eta_{n_\mu}(\mu)$ possesses a corresponding hyperbolic nodal structure. The nodal quantum numbers n_λ and n_μ are conserved for arbitrary parameter R. In the limit of large R (equivalent to the separated atom limit in molecular physics) the quantum numbers n_λ and n_μ coincide with parabolic coordinate quantum numbers n_1 and n_2 [7]. The effect of the outer electron is then to produce an electric field which is nearly constant over the spatial range experienced by the inner electron. Thus the inner wavefunctions merely become Stark-like states of the remaining He^+ ion.

The quantum analogue of the asymmetric (collinear) classical configuration of figure 1 consists of an inner electron in a molecular type state of maximal polarization along the axis $\mathbf{R}$. For a principal hydrogenic quantum number $N = n_\lambda + n_\mu + 1$ of the inner electron this implies $n_\lambda = 0$ (minimal off-radial excitation) and $n_\mu = N - 1$ (maximal number of nodes along $\mathbf{R}$).

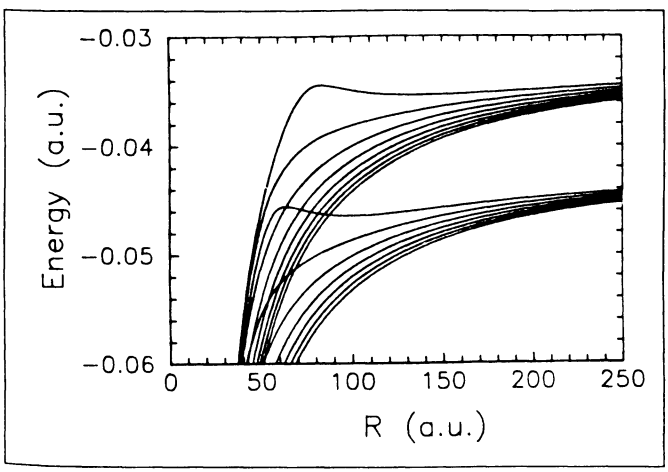

Figure 2: Born-Oppenheimer potential surfaces for the MO states (of helium) belonging to the $N = 7, 8$-manifold.

Figure 2 shows the series of Born-Oppenheimer potential curves

$$U_{n_\lambda n_\mu}(R) = \varepsilon_{n_\lambda n_\mu}(R) - \frac{Z}{R} \tag{4}$$

for all helium MO states belonging to the N=7,8–manifolds. $\varepsilon_{n_\lambda n_\mu}(R)$ denotes the energy eigenvalue of the two–center Hamiltonian. The potential curves for fixed N are labeled by n_λ and $n_\mu = N - n_\lambda - 1$ with n_λ running from zero (upper curve) to $N - 1$ (lower curve). As can be seen the upper potential curve of each N–manifold (in which the inner electron is maximally polarized along the axis $\mathbf{r}_1$) develops a broad potential well at $R \approx 100$ a.u. in figure 2. It is this minimum in the radial potential which leads to bounded vibrational motion of the outer electron. The solution of the radial Schrödinger equation for the outer electron in the BO potentials (4) yields the total energy of the three–body complex and (radial) wavefunctions for the motion of the outer electron. The wavefunctions of the vibrational motion of the slow electron in the outer potential well of the upper potential curves exhibit oscillator–like character. They are localized in the region of the outer potential minimum in close correspondence with the localized vibrational motion of the trapped 'classical' electron in figure 1(b). The (adiabatic) potential barrier corresponds to the dynamical barrier appearing in the classical solution and it prevents the outer electron from reaching the region around the nucleus.

For large R each MO manifold merges into a Stark multiplet as was discussed above and which can be seen explicitly in figure 2. The degree of polarization of the inner electron depends on N and n_λ. Only those MO curves in figure 2 which are related asymptotically to the Stark states of maximal orientation along the "field axis" $\mathbf{R}$ show a potential well. For $n_\lambda = 0$ and $N \geq 6$ the Born–Oppenheimer potentials show a minimum sufficiently pronounced to allow for quantized vibrational states. Below this value the off–radial extent of the inner electron MO wavefunction is too large. For the same reason wavefunctions with one or more nodal excitations perpendicular to $\mathbf{R}$ ($n_\lambda \neq 0$) do not support a potential minimum in figure 2. In general the occurrence of minima in the Born–Oppenheimer potentials is not restricted to MO states with n_λ=0. If N is large enough (i.e. $N \geq 16$ in the case of helium), the polarization of an inner–electron state with one off–radial node (n_λ=1) is strong enough to produce a potential well in the adiabatic potential.

For non–vanishing total angular momentum $\mathbf{L}$ the entire rotational energy of the three–body system leads to an additional raising of the adiabatic potential barrier and to a shift of the minima towards larger R. However, the overall structure is not affected.

Calculated energies for doubly excited states obtained within this single channel adiabatic approximation are compared with exact results in section V.

IV. AB INITIO CALCULATIONS

In this section we describe our numerical method to solve the Schrödinger equation for highly doubly–excited electron states. A full solution of this Schrödinger equation is a non–trivial problem. Here we use a transformation of the Schrödinger equation into perimetric coordinates [16, 17]. We obtain resonance

positions and resonance widths within near-machine precision even for highly excited states [9]. This allows us to check very accurately the predictions of the classical, semiclassical and adiabatic approximations described in the previous sections.

Using perimetric coordinates defined as [16,17]

$$x = r_1 + r_2 - r_{12} \quad ; \quad y = r_1 - r_2 + r_{12} \quad ; \quad z = -r_1 + r_2 + r_{12} \tag{5}$$

the Hamiltonian (1) for L=0 reads (with (x_1, x_2, x_3) defined as (x, y, z))

$$H = \frac{1}{(x+y)(x+z)(y+z)} \sum_{i,j=1}^{3} \frac{\partial}{\partial x_i} P_{ij}^{(3)}(x,y,z) \frac{\partial}{\partial x_j} - \frac{Z}{x+y} - \frac{Z}{x+z} + \frac{1}{y+z} . \tag{6}$$

The $P_{ij}^{(3)}$ are polynomials of degree 3 and can be found, e.g., in Ref. [18]. We expand each degree of freedom in a complete Sturmian basis set and (anti-) symmetrize the product functions. In this representation all the matrix elements are of simple analytical form. Their calculation requires mostly integer arithmetic and is fast and accurate. In addition, selection rules guarantee that most of them vanish. The resulting matrix equation is of banded, sparse structure and allows for efficient diagonalization.

We use the method of complex rotation [19, 20] to calculate accurate positions and decay widths of the autoionizing two-electron resonances. To give an estimate of the energy region covered by our calculations we note that doubly excited *intra*-shell resonances with N ranging from 6 to 18 cover this energy region. We diagonalize matrices up to dimensions of approximately 7000 to obtain an accuracy of the complex energies of at least 10 significant digits.

V. RESULTS

In table 1 we summarize our results for the energies of the resonant states ($^1S^e$ and $^3S^e$) which are described by the set of MO quantum numbers $(n_\lambda, n_\mu, \ell) = (n, 0, 0)$. The table gives the (numerically) exact results of the quantum calculations as well as the approximate values E_{scl} predicted by the simple semiclassical formula (2) and the approximate values E_{BO} obtained by solving the adiabatic single-channel equations with the adiabatic potentials supporting a minimum at large R ($n > 5$). States with $n \ll 6$ may be called precursors, since they possess a character that transforms smoothly into that of the high excited states.

As can be seen from table 1 the simple semiclassical formula is superior to the more elaborate adiabatic calculations in predicting accurately the quantum energies. The errors of the semiclassical energies are below 1% for all resonances (except the low lying $n = 2$ state of the $^1S^e$ subspace) and below 0.1% for states with $n > 7$.

Compared to energy eigenvalues, a direct examination of the nodal structure of the associated wavefunctions is a more stringent test of the different approximations. Figure 3(a) depicts the probability distribution of the wavefunction for the $(6, 0, 0)$ state of the principal series in the $(\Theta = 0)$-plane (Θ represents the

Table 1: Energies of the $(n,0,0)$ configurations obtained by full quantum solutions (singlet and triplet states respectively), the semiclassical triple Rydberg formula (2) (E_{scl}), and the single channel adiabatic approximation (E_{BO}). In addition the total decay widths obtained from complex rotation are given. (The numbers are truncated, not rounded).

n	$-E\,(^1S^e)$	$\Gamma/2\,(^1S^e)$	$-E\,(^3S^e)$	$\Gamma/2\,(^3S^e)$	E_{scl}	E_{BO}
2	0.257 371 609	0.000 010 564	0.249 964 615	0.000 006 789	0.247 923	-
3	0.141 064 156	0.000 011 739	0.140 088 483	0.000 004 409	0.139 351	-
4	0.089 570 804	0.000 002 024	0.089 467 826	0.000 000 179	0.089 144	-
5	0.062 053 558	0.000 000 560	0.062 041 278	0.000 000 033	0.061 887	-
6	0.045 538 667	0.000 000 202	0.045 539 242	0.000 000 376	0.045 458	0.045 956
7	0.034 842 642	0.000 000 368	0.034 843 857	0.000 000 143	0.034 798	0.035 109
8	0.027 517 599	0.000 001 184	0.027 519 289	0.000 000 022	0.027 491	0.027 612
9	0.022 284 587	0.000 000 525	0.022 283 665	0.000 000 035	0.022 265	0.022 413
10	0.018 411 985	0.000 000 058	0.018 411 896	0.000 000 030	0.018 400	0.018 507
11	0.015 468 259	0.000 000 023	0.015 468 265	0.000 000 019	0.015 460	0.015 541
12	0.013 178 121	0.000 000 022	0.013 178 140	0.000 000 010	0.013 172	0.013 235
13	0.011 361 442	0.000 000 014	0.011 361 444	0.000 000 005	0.011 357	0.011 406
14	0.009 896 121	0.000 000 004	0.009 896 120	0.000 000 002	0.009 893	0.009 932

angle between the electronic radial vectors). This corresponds to the collinear arrangement of the electrons. The off-collinear part of the probability density, not shown here, decreases exponentially indicating a zero point motion in the Θ-bending degree of freedom. The zero point motion is expressed by the assignment $n_\lambda = 0$ within the MO description respectively. The coordinate r_1 (r_2) denotes the radial distance of the outer (inner) electron. The outer electron probability is strongly localized in the region $r_1 \approx 120\,a.u.$, reflecting the dynamical localization of the "frozen" electron. Note also the large differences in the radial extents r_i. The nodal excitations are all directed along the periodic orbit of fig. 1, which is a nearly straight line along the radius of the frozen outer electron indicated by an arrow in the figure. Recalling the typical quadratic spacing of nodal lines in Coulombic systems, we achieve nearly constant nodal distances by using quadratically scaled axes as done in figure 3(d). The number of nodes along the orbit is $n = 6$ in agreement with the semiclassical predictions. The wavefunction does not show any off-orbit excitations, which agrees with the semiclassical local coordinate classification $(n,k,l) = (6,0,0)$.

Within the MO description the wavefunction is characterized as follows: The inner electron is maximally polarized along the nucleus–frozen electron–axis $\mathbf{R}$ ($n_\lambda = 0, n_\mu = 6$) while the outer electron is in its vibrational ground state ($\ell = 0$) of the effective potential well. Note the absence of nodal lines in r_1 for the exact wavefunction in figure 3(a). Thus the wavefunction reveals the equivalence of the semiclassical quantum number n and the MO quantum number n_μ.

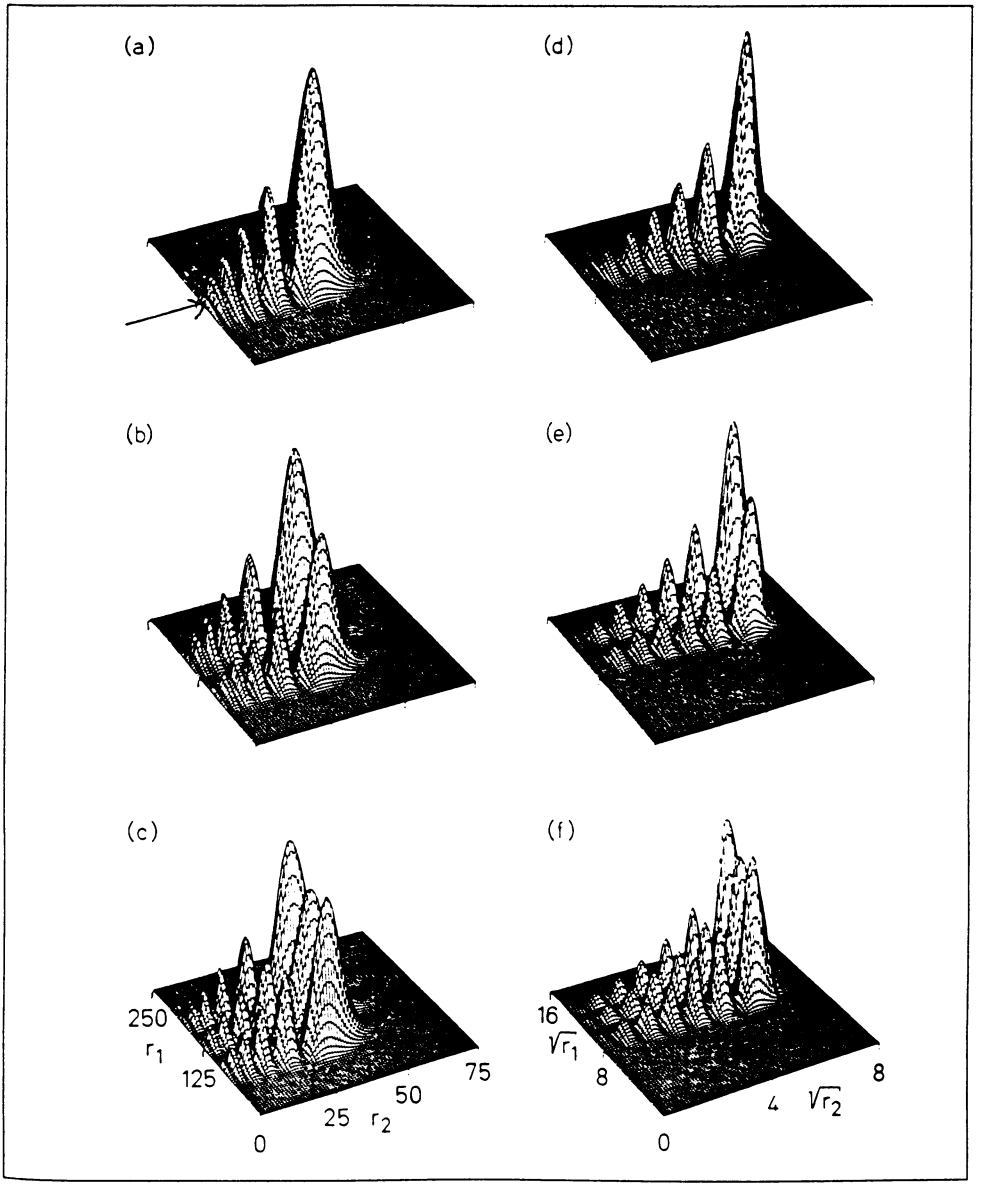

Figure 3: Conditional probability densities of $(n, 0, l)$ states in helium for n=6. The angle Θ between $\mathbf{r}_1$ and $\mathbf{r}_2$ is fixed to Θ=0. The axes have a linear (left part) and a quadratic scale (right part), respectively. Shown are l=0 (a,d), l=1 (b,e), and l=2 (c,f). Note the asymmetry in the scales of the axes. Only the parts $r_1 > r_2$ are shown. The full wavefunction is symmetric in r_1 and r_2.

The semiclassical triple Rydberg formula (2) suggests the existence of quantum states with nodal excitations transverse to the periodic orbit (labeled by l), which preserves the collinear character of the motion. Such configurations are shown in figure 3 for $l = 1$ (b,e) and $l = 2$ (c,f). In the adiabatic MO description such excitations in $r_1 = R$ represent vibrational levels of the outer electron. It follows that the quantum numbers l in the semiclassical and ℓ in the molecular classification scheme are identical.

Up to now we investigated the (radial) vibrational mode of the outer electron described by the quantum number l, i.e. excitations within the collinear arrangement of the electrons. We now focus on the structure of the inner electron wavefunction. In the adiabatic treatment the dynamics decouples into motion of the outer electron (vibrational R-motion) and of the inner electron, which for fixed R separates in prolate spheroidal coordinates λ, μ. To test these predictions we compare in figure 4 the probability densities of a two-center MO wavefunction of helium obtained within the adiabatic approach with the corresponding *ab initio* three-dimensional quantum wavefunction for fixed distances R of the outer electron. The figure then depicts the conditional probability for finding the inner electron in the coordinate space relative to the axis $\mathbf{R}$. We choose R as the classical expectation value for the radial distance of the outer electron along the classical periodic orbit of figure 1(a).

Part (a) of the figure 4 indeed shows that the inner electron wavefunction is of Stark-type character with maximal polarization along the axis between nucleus and outer electron. The state exhibits no off-radial excitations and is described by $n_\mu = 6, n_\lambda = 0$ in the MO classification scheme. A comparison of part (a) and (b) exhibits the close similarity of the approximate adiabatic and the full quantum wavefunction. This proves the validity of the adiabatic approximation and reveals the quasi-separability of the full quantum wavefunctions in molecular orbital coordinates. As shown in Ref. [10] full quantum wavefunctions with $n_\lambda \neq 0$ approximately separate in MO coordinates, too.

Finally, we focus on the correspondence between the classical and the quantum dynamics by showing in figure 5 a combined plot of the inner and outer electronic densities, which images the charge distribution of the entire two electron atom. A global space filling charge distribution is obtained by an overall rotation around the center of mass (nucleus). The probability density of the outer electron of the state $(6, 0, 0)$ is obtained in analogy to figure 4 by drawing a cut through the full wavefunction at a fixed radial distance r_2 of the inner electron. The wavefunction of the outer electron (left hand side of figure 5) appears as the bump far away from the nucleus Z. It just resembles the ground state oscillator-like wavefunction ($l = 0$) in the outer well of the BO-potential and turns out to be extremely non-hydrogenic. The inner wavefunction is taken from figure 4(b). These states exhibit strong electron correlation: *Radial* correlation leads to the oscillator-like wavefunction of the outer electron, *angular* correlation is visible from the polarized inner MO type wavefunction which is a coherent superposition of all

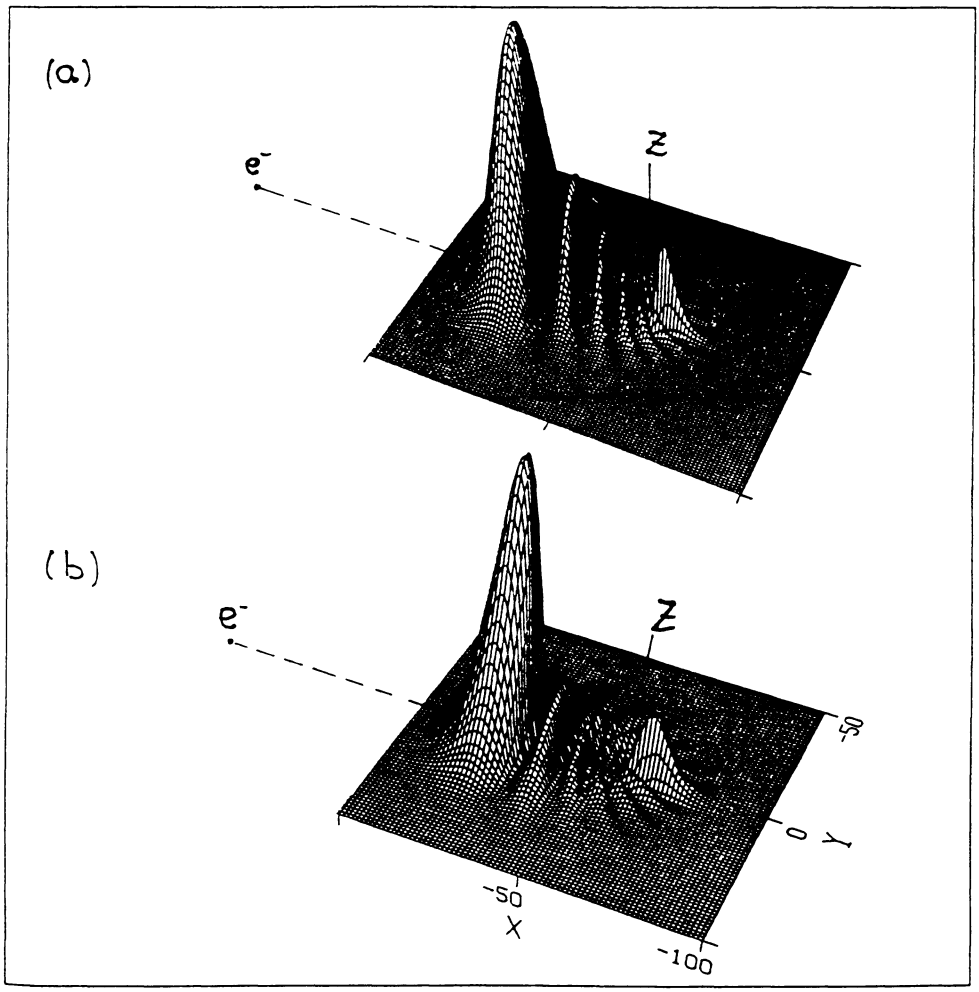

Figure 4: Conditional probability densities for the inner electron with respect to the fixed axis **R** between the nucleus and the outer electron. The $(n_\lambda, n_\mu, \ell) = (6,0,0)$ state obtained from the solution of the two-center Schrödinger equation within the Born–Oppenheimer approach (a) is compared with the corresponding *ab initio* quantum wavefunction (b). The position of the nucleus ($Z(=2)$) is indicated in parts (a) and (b). (Part (a) from Ref. [20]).

single–particle angular momenta l_i. A comparison with the quasiperiodic classical motion shown in figure 5(b) illustrates the classical–quantal correspondence of the electron–pair motion.

There are in principal two mechanisms which lead to decay of the planetary configurations described in the preceding sections: radiative and non–radiative

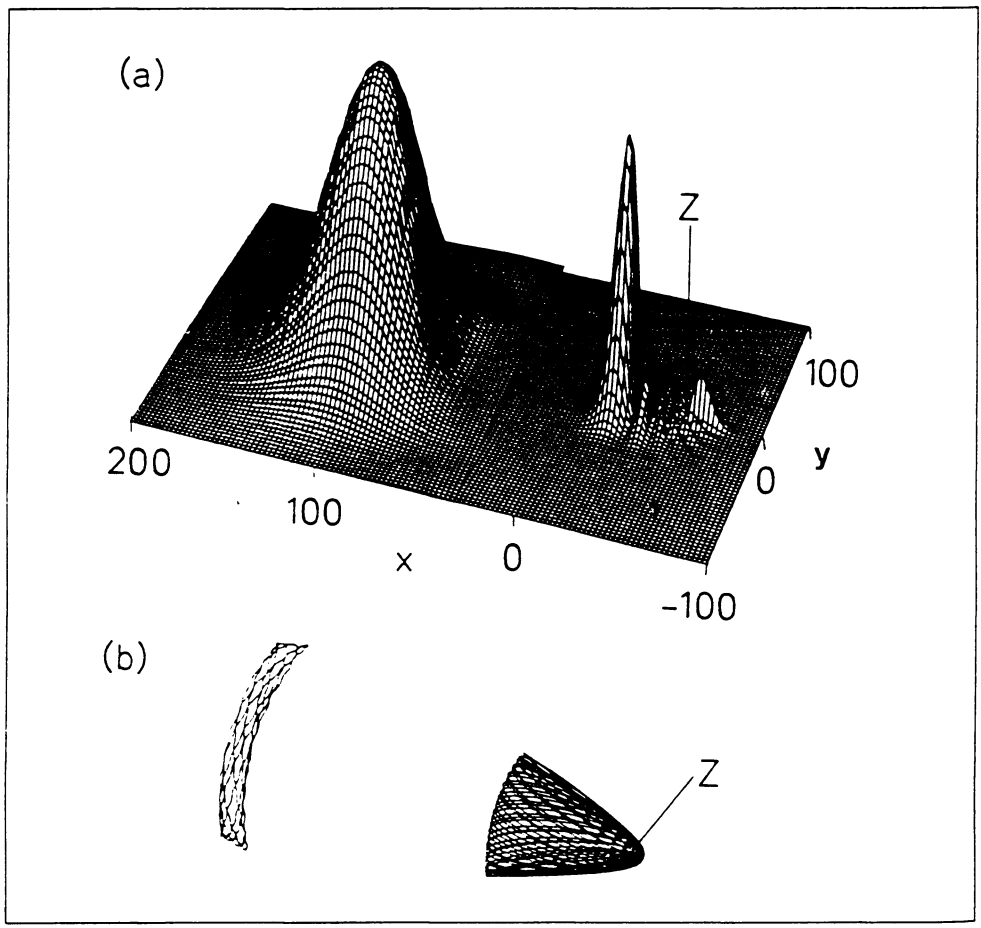

Figure 5: Image of the charge distribution of the helium atom in the $(6,0,0)$ state, part (a). The right part is the probability distribution of the inner electron at fixed radial distance R of the outer electron; the left part is the probability for the outer electron at fixed inner electron radius r_2. The fixed values were chosen as the classical outer turning points of the electrons. Part (b) shows a typical classical trajectory of the two electrons. The trajectory is confined to a torus in phase space. The position of the nucleus (Z) is indicated in part (a).

decay. We will focus on non–radiative particle decay, i.e. autoionization of the resonances. Since the classical motion corresponding to the quantum states is stable (see figure 1) they are classically bound. However, in analogy to the (semiclassical) penetration through a "static" potential barrier these states can autoionize semiclassically by "dynamical" tunneling [22], but the decay widths for such processes decrease exponentially with the nodal excitation along the orbit [10].

In table 1 we summarize the widths of the ${}^1S^e$ and ${}^3S^e$ resonances with quantum numbers $(n,0,0)$. They were calculated fully quantum mechanically using the complex rotation method (section IV). The imaginary parts are extremely small. The widths $\Gamma/2$ indeed decrease exponentially with increasing nodal excitation $n \sim 1/\sqrt{-E}$, $\ln \Gamma/2 \simeq -0.71\, n$, although they fluctuate rather strongly around the average trend. Thus the resonances appear as bound states in the continuum in the limit of large excitation even though the number of open channels increases tremendously with increasing energy (more than 100 channels are open for the $n = 14$ state!).

VI. CONCLUSION

In the present work we have studied properties of a certain class of correlated resonant states of two-electron atoms and ions of highly doubly-excited electrons. The problem has been investigated from several different points of view — classically, semiclassically and quantum mechanically (both exactly and in an adiabatic approach). Summarizing the results we have established a classification of these resonant states in terms of semiclassical quantum numbers (n,k,l) associated with local coordinates of the periodic orbit and the MO set (n_μ, n_λ, ℓ) associated with molecular-type coordinates, which (locally) are identical. The exact wavefunctions of the problem show quasi-separable behaviour in these coordinates. The corresponding underlying dynamical symmetry appears due to the distinct electron correlation. Energies calculated within the two approximate approaches reproduce the exact quantum results quite accurately.

The resonant states possess extremely small widths which decrease exponentially with increasing excitation.

An alternative approach would be to look for similar configurations in other three-body systems. It is immediately obvious from the classical analysis that the dynamically localized outer electron can be replaced by heavy negatively charged particles (such as kaons K^- or antiprotons $\bar{p}$) without changing inner electron dynamics essentially. Indeed, the present mechanism has been proposed as a trap for anti-particles [23] and unexpectedly long-lived states have been found experimentally in such systems recently [24].

ACKNOWLEDGMENTS

We would like to thank J S Briggs, E A Solov'ev, U Eichmann, J M Rost, W Sandner and R Thürwächter for stimulating discussions. This work was supported by the Deutsche Forschungsgemeinschaft under contract Wi877/2 and within the Sonderforschungsbereich 276 at the University of Freiburg.

REFERENCES

[1] Camus P, Gallagher T F, Lecomte J M, Pillet P and Boulmer J, Phys. Rev. Lett. **62**, 2365 (1989)

[2] Eichmann U, Lange V and Sandner W, Phys. Rev. Lett. **64**, 274 (1990), Phys. Rev. Lett. **68**, 21 (1992)

[3] Sandner W, this volume

[4] Hogervorst, this volume

[5] Fano, U, Phys. Rep. **46**, 97 (1983)

[6] Herrick D E, Adv. Chem. Phys. **52**, 1 (1983)

[7] Rost J M and Briggs J S, J. Phys. B **24**, 4293 (1991)

[8] Green, C H, this volume

[9] Richter K and Wintgen D, J. Phys. B **24**, L565 (1991)

[10] Richter K, Briggs J S, Wintgen D and Solov'ev E A, J. Phys. B, in press (1992)

[11] Percival I C, Proc. Roy. Soc. Lond. A **353**, 289 (1977)

[12] Ezra G S, Richter K, Tanner G and Wintgen D, J. Phys. B **24**, L413 (1991)

[13] Gutzwiller M C, *Chaos in Classical and Quantum Mechanics* (New York: Springer) (1990)

[14] Richter K and Wintgen D, Phys. Rev. Lett. **65**, 1965 (1990)

[15] Helfrich K, Theor. Chim. Acta **24**, 271 (1972)

[16] James H M and Coolidge A S, Phys. Rev. **51**, 857 (1937)

[17] Pekeris C L, Phys. Rev. **112**, 1649 (1958)

[18] Zhen Z, Phys. Rev. A **41**, 87 (1990)

[19] Reinhardt W P, Ann. Rev. Phys. Chem. **33**, 223 (1982)

[20] Ho Y K, Phys. Rep. **99**, 1 (1983)

[21] Thürwächter R, private communication (1992)

[22] Davies M J and Heller E J, J. Chem. Phys. **75**, 246 (1981)

[23] Richter R, Rost J M, Thürwächter R, Briggs J S, Wintgen D and Solov'ev E A, Phys. Rev. Lett. **66**, 149 (1991)

[24] Iwasaki M et al., Phys Rev. Lett. **67**, 1246 (1991)